

Bio-enzyme pretreatments for anaerobic co-digestion of food waste blended with bioplastics: Effects on methane production and microbial community structure

Xintong Jiang ^{a,b}, Dongsu Bi^a, Yu Cheng^{a,b}, Shizhuo Wang^b, Bo-yu Peng^d, Haowen Shen^b,
Tao Zhang^{c,*}, Xuefen Xia^b, Zheng Shen^{b,*} and Yalei Zhang^d

^a School of Chemical and Environmental Engineering, Shanghai Institute of Technology, Shanghai 201418, China

^b Institute of New Rural Development, Tongji University, Shanghai 200092, China

^c College of Design and Innovation, Tongji University, Shanghai 200092, China

^d State Key Laboratory of Pollution Control and Resource Reuse, College of Environmental Science and Engineering, Tongji University, Shanghai 200092, China

* Corresponding Authors

E-mail: shenzheng@tongji.edu.cn:

E-mail: zt1814@aliyun.com

Supplementary Methods

M1. Detailed procedures for anaerobic fermentation

According to Yu, Dongsu et al. (2022), anaerobic co-digestion of three commercial bioplastic bags with food waste effects on methane production and microbial community structure, (2020). All experiments were conducted using the batch method using a 150 ml pipe jaw headspace bottle as the reactor with an effective working volume of 70 ml. Two experimental groups were designed based on temperature: a mesophilic group(35°C) and a thermophilic group(55 °C). The content of CH₄ was determined in the experiments of anaerobic fermentation, and the composition of the generated gas was determined by GC8860 gas chromatograph with a capillary column HP-PLOT/Q (30m×0.530mm×40μm), with Ar as the carrier gas, a column flow rate of 8 mL/min, a pressure of 8.438 psi, a split ratio of 3:1, and a thermal conductivity detector (TCD) for detection and analysis, with an injection port temperature and column temperature of 60°C, a detector temperature of 200°C, and a sample volume of 0.2 ml. The content of CH₄ was calculated using the area regression method.

M2. The source of bioplastics

According to Yu, Dongsu et al. (2022)'s conclusions, the methane production rate of the three bioplastics under both mesophilic and thermophilic conditions indicated that PBAT/PLA/starch>PLA>PBAT.

M3. Detailed procedures for scanning electron microscope (SEM) and Fourier transform infrared spectroscopy (FTIR)

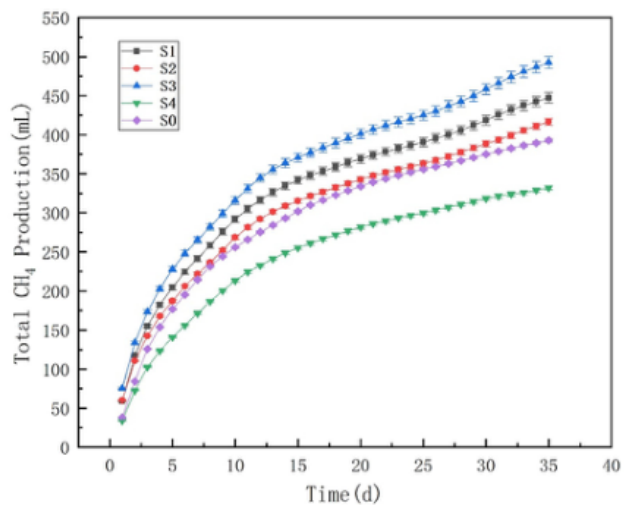
According to Yu, Dongsu et al. (2022)'s experiment, after 35 days of anaerobic co-fermentation with food waste, samples of the four different plastic materials were collected from the reactor, washed repeatedly with distilled water, dried at 28-30°C, and used immediately inspected by scanning electron microscopy and Fourier transform infrared spectroscopy.

M4. Detailed procedures for Microbial analysis

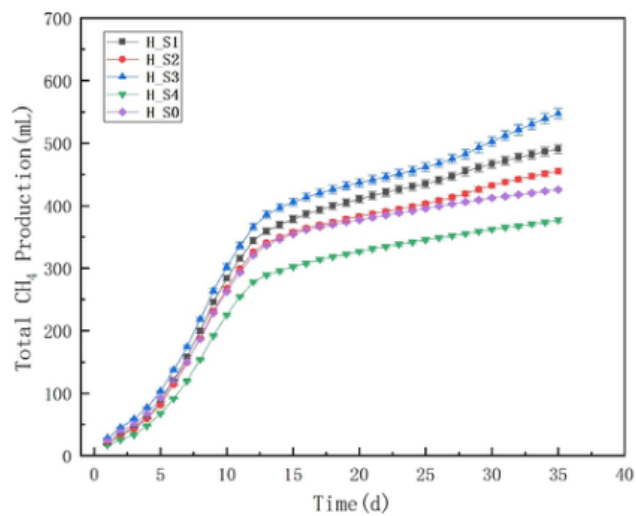
According to Yu, Dongsu et al. (2022)'s experiment, at the conclusion of the experiment, serum bottles were shaken to mix evenly, and a minimum of 10 ml of sludge from each was placed in separate 50 ml centrifuge tubes and spun at 4000 rpm for 5 minutes. The supernatant was discarded, and the remaining sediment was stored in a sterile centrifuge tube and stored on dry ice until they could be sent to Shanghai Meiji Biomedical Technology Company for analysis. The bacterial 16S rRNA gene was amplified in the V3-V4 region with specific primers. The F-terminal sequence was ACTCCTACGGGAGGCAGCAG, and the R-terminal sequence was GGACTACHVGGGTWTCTAAT (Xu et al., 2016). For archaea, the F-terminal sequence was FGYCAGCCGCCGCGGTAA, and the R-terminal sequence was YCCGGCGTTGAVTCCAATT (Liu et al., 2016). After extracting the genome of the

sample, the yield and purity of DNA were determined, and following PCR amplification, the product was purified, and IlluminaMiseq was used for high-throughput sequencing.

Supplementary Figures



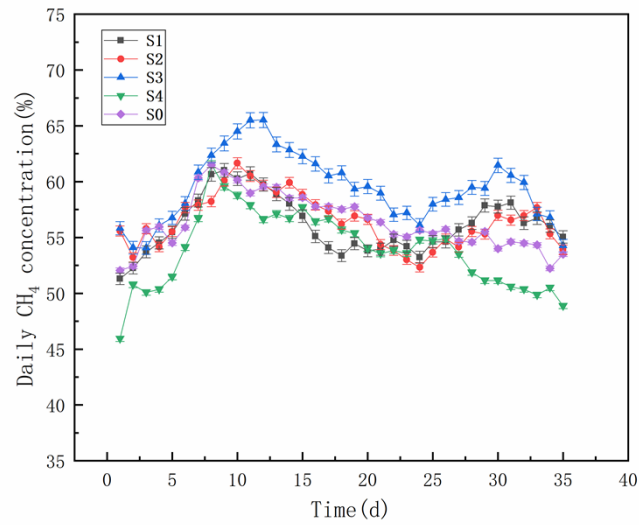
(a)



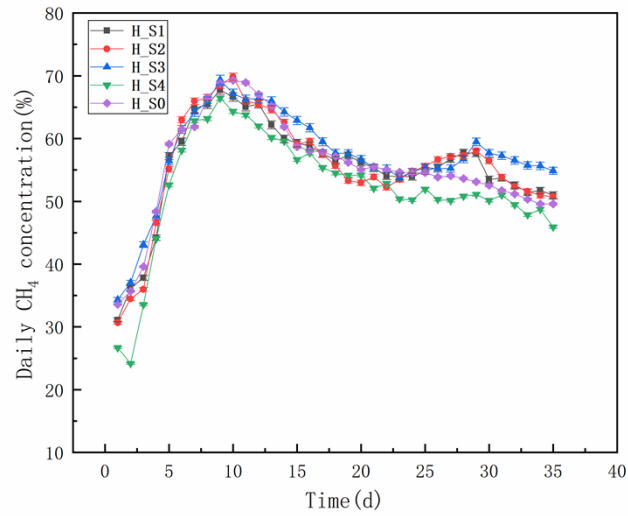
(b)

Figure S1. Cumulative CH₄ production: (a) 35°C conditions (S3 PBAT/PLA/starch); (b) 55°C conditions(H_S3 PBAT/PLA/starch)

Note: The bioplastics selected in the manuscript are group S3 and H_S3 in the above figure as the basis for selection, corresponding to medium temperature and high temperature respectively. The methane production rate is optimal for this type of bioplastic bag during anaerobic fermentation.



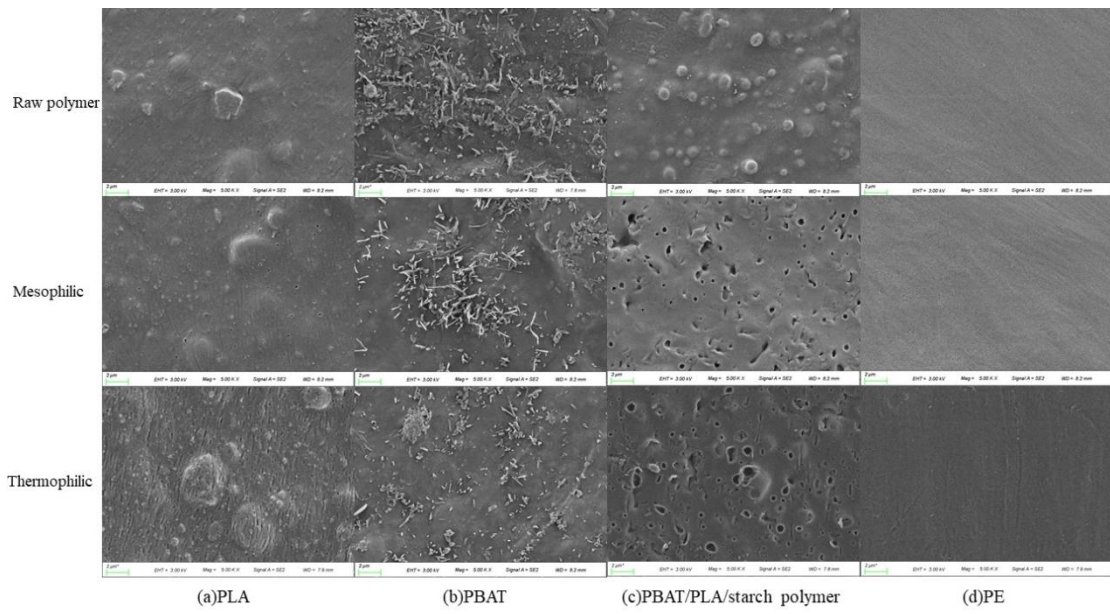
(a)



(b)

Figure S2. Daily CH₄ ratio during anaerobic digestion: (a) 35°C conditions (S3 PBAT/PLA/starch); (b) 55 °C conditions (H_S3 PBAT/PLA/starch)

Note: The bioplastics selected in manuscript are group S3 and H_S3 in the above figure as the basis for selection, corresponding to medium temperature and high temperature respectively. The second methane concentration peak appeared on the 30th and 29th days, respectively.



Fig

re S3. SEM images of the four plastics before and after anaerobic co-fermentation

Note: The bioplastics selected in the manuscript are group (c) PBAT-PLA/starch polymer

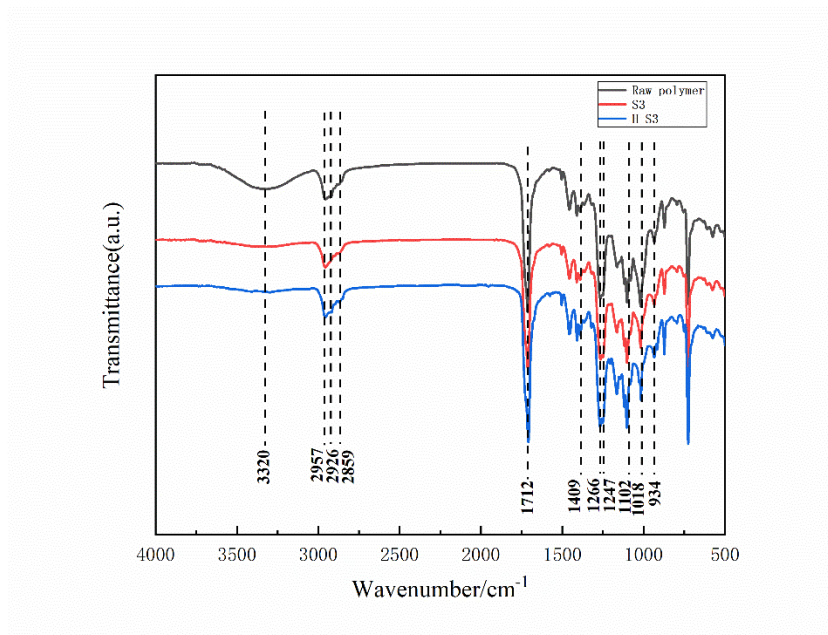


Figure S4. FTIR spectra of the three degradable plastics before and after anaerobic co-fermentation: PBAT/PLA/starch (S3 35 °C condition; H_S3 55 °C condition)

The microbial diversity indices, including the Shannon value and Simpson value, collectively reflected the diversity of the sample community. (Grehs, Lopes et al. 2019). Rarefaction curves with a Shannon Index at the OTU level were generated for all samples. The changes in intestinal microbial diversity were confirmed via analysis of the Shannon Index (Figure S5 and Table S1). The significant increase in the Shannon Index (from 4.41373 to 4.5407 for Bacterial, and from 1.63375 to 2.17662 for Archaeal, $p < 0.0001$) suggested higher microbial diversity at 55 °C. This increase in diversity is likely due to the adaptation of most mesophilic anaerobes to higher temperatures. It can be presumed that the microbiota approached a biodegradation-functionalized community with the addition of proteinase K at 55 °C after 35 days of anaerobic digestion. Chao index values and ACE index values can effectively reflect the richness of species in the samples (Alessandri, Milani et al. 2019). The diversity of archaeal communities was higher at 55 °C, possibly due to the elevated temperature being more suitable for the growth of a greater number of archaea. Conversely, the richness of bacterial species in the samples at 35 °C was higher than at 55 °C. This is likely because the high-temperature sludge was domesticated from medium-temperature sludge, causing some bacteria that were adapted to medium temperatures to die during the adaptation process. (Jangsen, Mengnan et al. 2020). Bacterial and archaeal samples reached

plateaus at around 20,000 reads and 13,000 reads, respectively. The results also revealed that archaea at 55 °C exhibited steeper rarefaction curves and higher taxonomic richness compared to those at 35 °C, while the opposite was observed for bacteria. (Figure S6). at were adapted to medium temperatures to die during the adaptation process. (Jangsen, Mengnan et al. 2020). Bacterial and archaeal samples reached plateaus at around 20,000 reads and 13,000 reads, respectively. The results also revealed that archaea at 55 °C exhibited steeper rarefaction curves and higher taxonomic richness compared to those at 35 °C, while the opposite was observed for bacteria. (Figure S6).

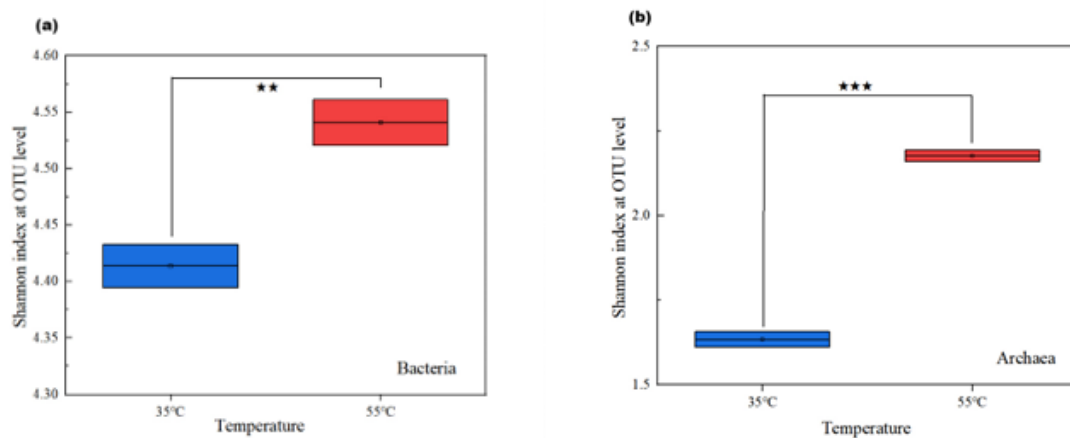


Figure S5. Analysis of microbiome post-reaction after proteinase K pretreatment substrate sludge. Shannon Index of microbial communities. *** indicate statistical significance ($p < 0.0001$). (a) bacterial; (b) archaeal

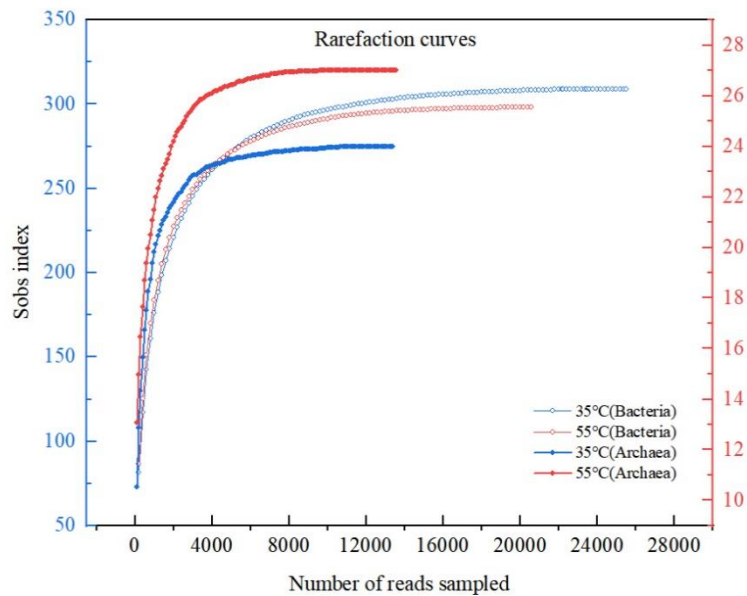
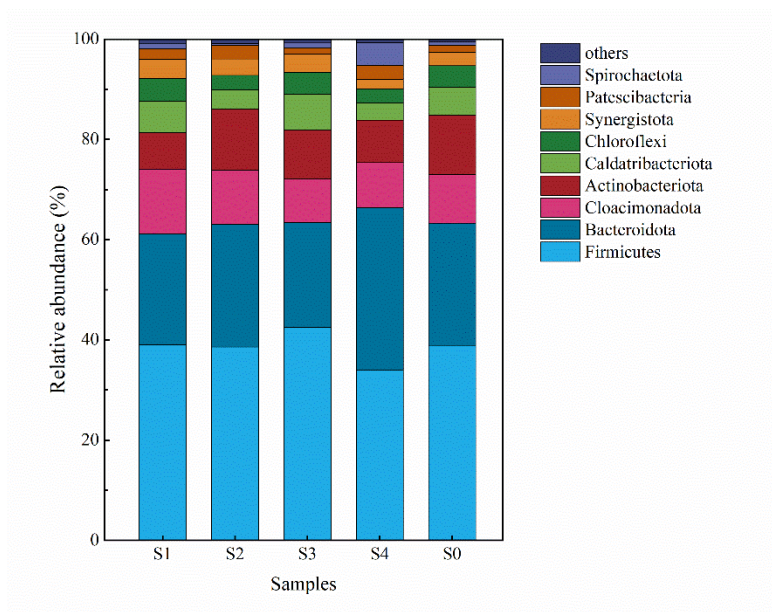
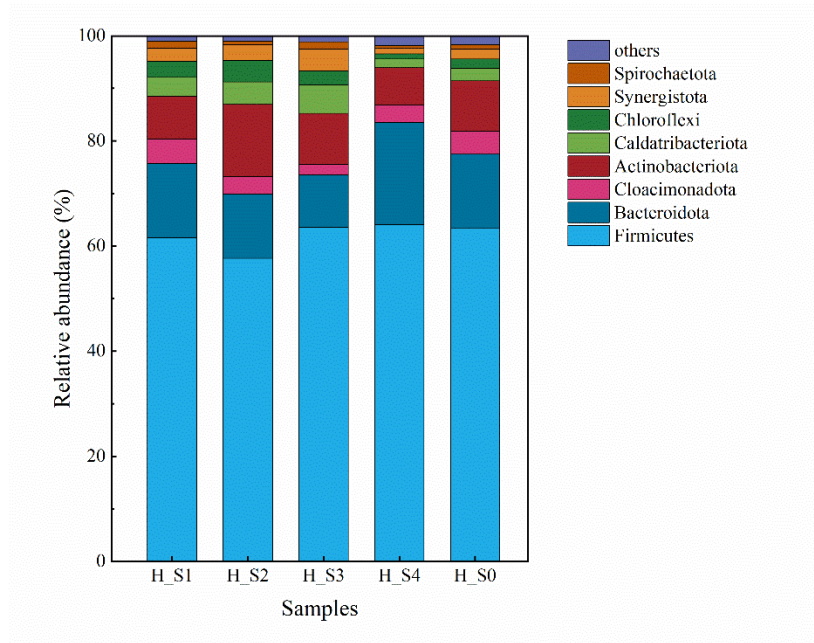


Figure S6. Analysis of microbiome in post-reaction substrate sludge. Shannon Index of microbial communities. *** indicate statistical significance ($p < 0.0001$). (a) bacterial; (b) archaeal

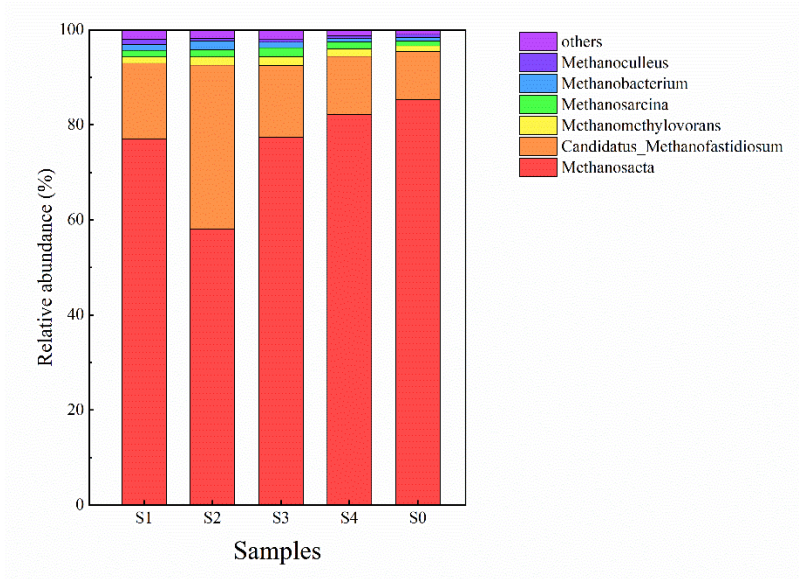


(a)

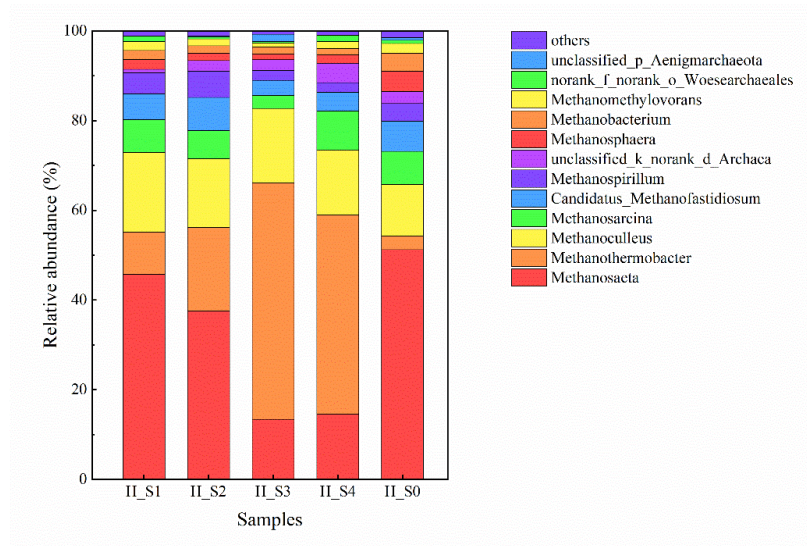


(b)

Figure S7 Bacteria community structure at the phylum level: (a) following mesophilic digestion; (b) following thermophilic digestion



(a)



(b)

Figure S8. Archaea community structure at the genus level: (a) following mesophilic digestion; (b) following thermophilic digestion

References:

Alessandri, G., C. Milani, L. Mancabelli, M. Mangifesta, G. A. Lugli, A. Viappiani, S. Duranti, F. Turroni, M. C. Ossiprandi, D. van Sinderen and M. Ventura (2019). "Metagenomic dissection of the canine gut microbiota: insights into taxonomic, metabolic and nutritional features." Environ Microbiol **21**(4): 1331-1343.

Grehs, B. W. N., A. R. Lopes, N. F. F. Moreira, T. Fernandes, M. A. O. Linton, A. M. T. Silva, C. M. Manaia, E. Carissimi and O. C. Nunes (2019). "Removal of microorganisms and antibiotic resistance genes from treated urban wastewater: A comparison between aluminium sulphate and tannin coagulants." Water Research **166**: 115056.

Jangsen, C., C. Mengnan, P. E. Poh, J. D. Ocon, M. Z. H. Md Zoqratt and S. M. Lee (2020). "Impacts of morphological-controlled ZnO nanoarchitectures on aerobic microbial communities during real wastewater treatment in an aerobic-photocatalytic system." Environmental Pollution **259**: 113867.